# New insights into cathepsin D in mammary tissue development and remodeling

Naira V. Margaryan,[1] Dawn A. Kirschmann,[1,2] Alina Lipavsky,[1] Caleb M. Bailey,[3] Mary J.C. Hendrix[1,2] and Zhila Khalkhali-Ellis[1,2,*]

[1]Children's Memorial Research Center; Cancer Biology and Epigenomics Program; [2]Robert H. Lurie Comprehensive Cancer Center; Northwestern University Feinberg School of Medicine; Chicago, Illinois USA; [3]The Stowers Institute for Medical Research; Kansas City, MO USA

Cathepsin D (CatD) is a lysosomal aspartyl endopeptidase originally considered a "house keeping enzyme" involved in the clearance of unwanted proteins. However, recent studies have revealed CatD's involvement in apoptosis and autophagy, thus signifying an important function in the proper development and maintenance of multi-cellular organs.

In the mammary gland, matrix degradation and the remodeling process are orchestrated by proteolytic enzymes, but the role of CatD at distinct developmental stages has remained mostly unexplored. Based on our previous studies we sought to address the role of this endopeptidase in mammary gland development and remodeling. By employing a mouse model, we report a previously unidentified participation of CatD in different stages of mammary gland development. Our findings reveal that CatD undergoes distinct protein processing at different stages of mammary gland development, and this customized processing results in differential enzymatic activity (constitutive and low pH activatable) best fitting particular stage(s) of development. In addition, at the onset of involution the N-glycan structure of this endopeptidase switches from a mixed high mannose and hybrid structure to an almost exclusively high mannose type, but reverts back to the original N-glycan composition by day 4 of involution. Our findings illuminate (at least in part) the "raison d'être" for CatD's numerous and highly regulated proteolytic processing steps from the pro-form to the mature enzyme. In the mammary gland, specific cleavage product(s) perform specialized function(s) befitting each stage of remodeling.

It is noteworthy that deregulated synthesis, secretion and glycosylation of CatD are hallmarks of cancer progression. Thus, identifying the role of CatD in a dynamic normal tissue undergoing highly regulated cycles of remodeling could provide valuable information illuminating the deregulation of CatD associated with cancer development and metastasis.

## Introduction

The dynamic structure of mammary tissue undergoes frequent and highly regulated cycles of remodeling during a female's life. During puberty, proliferation and remodeling at the terminal end bud drives the morphogenesis of the epithelial duct system. Ductal extension is supported by proliferation and sculpting the hollow tube of the subtending duct, accomplished in part through apoptosis.[1] Pregnancy causes a radical expansion and reorganization of the epithelial alveolar compartment to prepare the mammary gland for lactation.[2] Parturition, which is associated with a drop in serum progesterone levels, activates the onset of milk secretion.[3,4] In the absence of suckling, milk accumulates in the alveolar lumens, thus triggering a decline in systemic lactogenic hormones[5] and heralds the necessity for involution. The involution process occurs in two distinct stages: In the first stage (reversible), alveolar cells undergo programmed cell death, but there is no remodeling of the lobuloalveolar structure. In the second stage (non-reversible), the coordinated action of proteinases degrades basement membrane and extracellular matrix (ECM) and disrupts the lobuloalveolar structure[6] to return the gland to a state comparable to virgin stage.[7] The gene expression and proteomics profile associated with each stage of development and remodeling have been extensively studied and facilitated by defining changes at the transcriptional and translational levels.

Cathepsin D (CatD) is an aspartyl endopeptidase expressed in all living cells with the exception of red blood cells. It is synthesized as a pre-pro-enzyme in the endoplasmic reticulum,[8] glycosylated, and then transported to the Golgi and ultimately to the endosomal/lysosomal compartment. This endopeptidase is subjected to successive and highly regulated proteolytic cleavages to form the mature active 32 and 14 kDa chains in the acidic pH of the lysosomes.[9,10] CatD is also secreted as a pro-enzyme and can be activated by auto-activation, cleavage by other proteases or upon exposure to an acidic environment. Although CatD's original function was believed to be mostly the intercellular clearance of proteins, recent studies have indicated CatD's involvement in apoptosis[11,12] and autophagy,[13-15] thus signifying

its important role in the proper development and maintenance of multi-cellular organs. However, the underlying molecular role of CatD in mammary gland development and the remodeling process has not been addressed previously. We hypothesized that in the mammary gland CatD expression is temporally and spatially regulated and its function at distinct stages of remodeling is controlled by precise post-translational protein processing. To test our hypothesis we utilized the mouse mammary gland at different developmental stages and examined the protein profile, enzymatic activity and oligosaccharide composition of this multi-faceted endopeptidase. This approach has illuminated a previously unidentified involvement of CatD at each stage of mammary gland development and remodeling. In addition, the findings reveal that a precisely regulated differential processing, glycosylation and activity of CatD are tailored for each stage of mammary gland remodeling, thus providing new insights into a well known aspartyl endopeptidase—with significant implications for cancer development and metastasis.

## Results

To address the role of CatD in mammary gland development and remodeling we utilized a mouse model and extracted mammary glands from virgin, pregnant, lactating and post-lactating (involuting) animals. Initially, we examined the protein expression profile of CatD by immunohistochemical analysis of formalin fixed tissue. This approach indicated that CatD is expressed by mammary epithelial cells at all stages of remodeling and its level increases with the development of the glands from virgin to secretory glandular structures (**Fig. 1**). In the latter, CatD is mostly at the apical surface of the polarized epithelia and is abundantly detected in the milk at early lactation but decreases as lactation progresses. At the onset of involution, and despite the abundant presence of milk in the lumen, the CatD immunostaining is mostly restricted to the glandular structures and minimally detected in the milk filled lumen (**Fig. 1 and Suppl. Fig. 1**). Interestingly, at involution day 2 the CatD levels in the milk increases and the staining profile of the glandular epithelial layer resembles a honeycomb pattern (some hollow and some with densely stained cellular material) with intense focal staining around the "combs" (**Fig. 1** and arrows). With advancing involution the honeycomb structures are more frequent and the matrix is visibly remodeled (**Fig. 1 and Suppl. Fig. 1**). It is important to note that maximal CatD immunoreactivity is detected at involution days 2–4, and by day 15 the epithelial structure resembles that of virgin stage.

As an indicator of functional secretory alveoli, expression of milk protein WAP was investigated which indicated its exclusive apical association and maximal level at involution days 1 and 2 (**Suppl. Fig. 2**). By involution day 7, WAP immunostaining was only observed in the ductal secretion.

The involvement of CatD in mammary gland remodeling was further examined using an in vitro model of acini formation in the 3-D organotypic culture. In this model, the acini possess a spherical architecture similar to that observed in vivo.[16] At early stages of growth, considerable CatD immunoreactivity is associated with the matrix juxtaposed to the developing acini (**Fig. 2A**). As the acini mature CatD immunoreactivity can also be detected in the hollowing inner structure forming the lumen (**Fig. 2B**).

CatD is synthesized as a pre-pro-enzyme and undergoes several highly regulated proteolytic cleavages to yield the mature active enzyme. By employing western blot analysis of the post-nuclear cytosolic fractions of the mammary gland we noted that CatD protein processing from the pro-form to ultimately the mature form(s) varies at all stages. The pro- (~47 kDa), the intermediary- (~43 kDa), the active single chain (~41 kDa) and the mature form (~32 kDa) are detected at comparable proportions in virgin, pregnant and early lactating glands, with maximal CatD expression observed at early lactation and decreasing
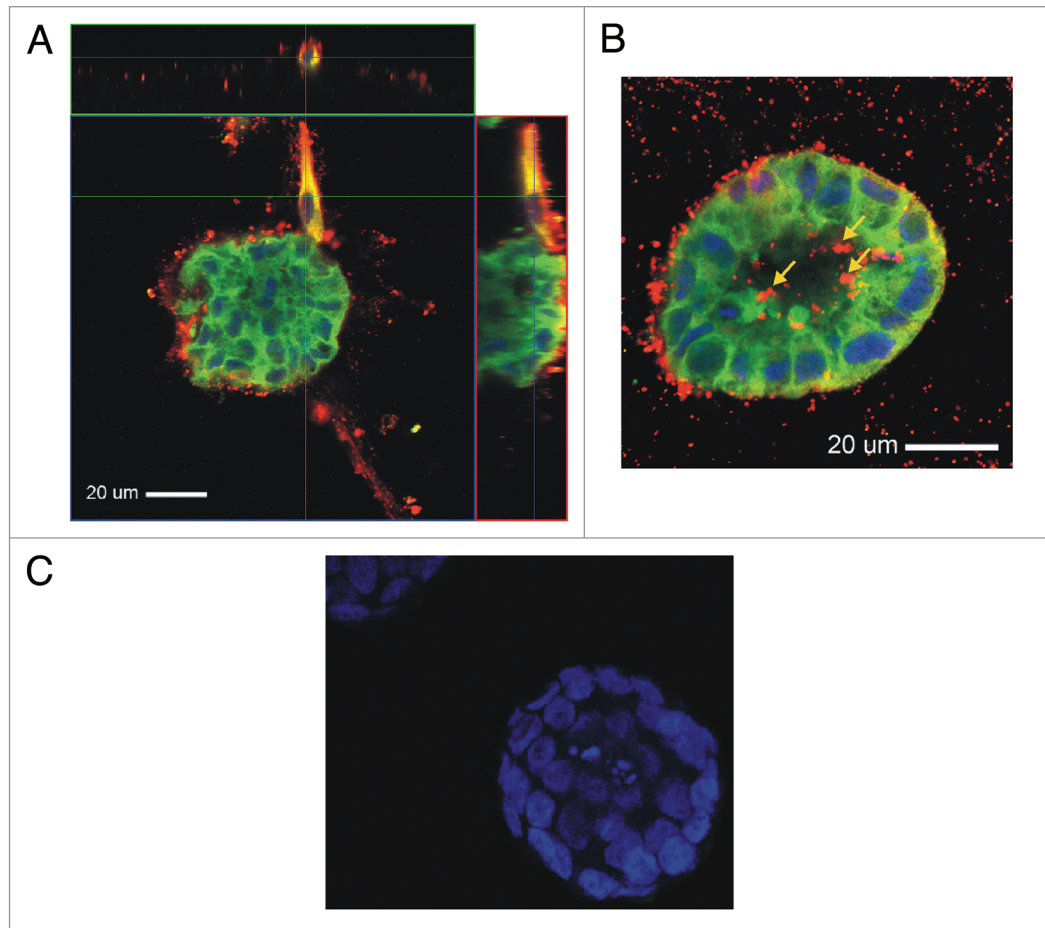
**Figure 2.** CatD expression in the developing acinus. MCF-10A cells were grown on 3-D basement membrane cultures to form hollowed spheres resembling mammary lobular structures. Acini at different maturation points (4 and 7 days in culture, A and B, respectively) were fixed for immunofluorescence analysis. CatD immunostaining is depicted in red and indicated by arrows; Maspin (an epithelial marker protein) is in green and nuclei are stained with DAPI (blue). The presence of CatD on the surface of acini is determined by Z stacking of the confocal image in (A). The specificity of antibodies is examined using no primary and depicted in (C). Original magnification, x63.

thereafter (**Fig. 3A**). The onset of involution prompts a rise in CatD with a prominent presence of the ~47 kDa form which now bears a slightly higher molecular mass (**Fig. 3A**). This elevated mass persists through involution day 3 but is back to normal by day 4 involution. By day 2 involution apart from the considerable increase in CatD level, the cleavage to the active 32 kDa single chain resumes and elevates exponentially by day 4 involution. The 47 kDa pro-form could no longer be detected at day 4 involution. By day 15 involution, the CatD protein profile almost resembled that associated with the virgin stage. Analysis of the milk samples from involution days 1 and 2 indicated a very limited presence of the 41 kDa band in the milk samples and generally a much lower level of CatD in the involution day 1 milk compared to that of day 2 (**Fig. 3B**), thus further supporting our immunohistochemical observation (**Fig. 1**).

Based on the observed differential protein processing, we sought to examine the possible differences in CatD enzymatic activity (total activity, constitutively active and low pH activatable CatD) in these stages of development. We observed that virgin, pregnant and early lactating glands exhibited high levels of total

CatD activity with comparable intensity (**Fig. 4A**). By lactation days 7 and 15, total CatD activity had dropped by ~20 and 80%, respectively, when compared to lactation day 1. CatD total activity at day 1 and to some extent day 2 involution was comparable to that of lactation day 15 but rose dramatically by day 3 and 4 involution. Particularly noteworthy is the level of mature 32 kDa (and 14 kDa) form(s) reflecting constitutive activity in involution days 3, 4, 15, virgin and pregnant stages. The low pH activatable CatD levels differed greatly at all stages: Early lactation presented with the highest level of low pH activatable CatD (up to 80% of total CatD), compared to ~43% and 64% in virgin and pregnant glands, respectively (**Fig. 4B and Table 1**). However, progression to late lactation was associated with a rapid decline in the activatable CatD (61% and 32% in lactation day 7 and 15, respectively), which reached its lowest level at the onset of involution (9.3%). Advancing involution was associated with a dramatic increase in the constitutively active form (**Fig. 4B and Table 1**). The involution day 1 milk sample had minimal constitutively active CatD, which increased slightly by day 2 involution (**Fig. 4C**).
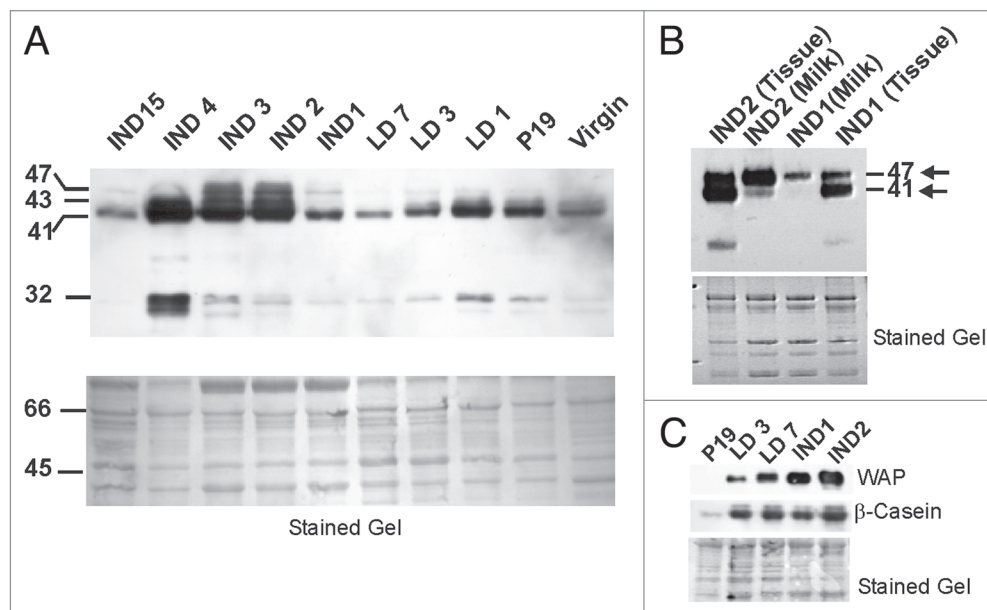
**Figure 3.** CatD protein expression profile at different stages of mammary tissue development. For this analysis 30 μg total protein of the post-nuclear cytosolic extracts (as described in the Materials and Methods) was subjected to SDS-PAGE (12.5% resolving gel) and western blot analysis using a mouse specific antibody to CatD (A). Comparison of the CatD protein profile of milk from involution days 1 and 2 with its comparable tissue extracts is depicted in (B). The molecular mass of CatD pro-form (~47 kDa) and its processed products (43, 41 and 32 kDa) are indicated in the figure. As markers of functional secretory alveoli, the expression profile of milk proteins WAP and β-casein are also depicted in (C). (Due to the high abundance of WAP protein, the blots were exposed for a much shorter time frame compared to that of β-casein). All conditions in (C) were the same as in (A) except the SDS-PAGE was performed on a gradient of 4–12.5%. For the loading control, the stained gel following the transfer is included for (A–C). Arrows indicate the position of the pro- (~47 kDa) and active single chain (~41 kDa) CatD.

CatD is a glycosylated enzyme with two N-linked oligosaccharides (N-glycans) on its asparagine (Asn) residues 70 and 199 (**Suppl. Fig. 3**). Thus, we sought to examine the possible variability in the N-glycan structures associated with any specific developmental stage by employing two enzymes: PNGase F (to cleave the Asn-GlcNAc bond and thus release all types of N-glycan structures) and endo-H (to release the high mannose but not complex structures). We observed that the 47 and 41 kDa bands exhibit comparable mixed N-glycan profiles at virgin, pregnant and late involution (**Fig. 5A–C**). However, at involution day 1 the N-glycan structure(s) on the 47 and 41 kDa bands were almost exclusively of the high mannose type; this profile reverted back to the mixed structures by day 3 involution (**Fig. 5A–C**). To verify this intriguing finding we examined the expression profile of glycosyl transferase responsible for the formation of hybrid and complex N-glycan structures MGAT 1 (mannosyl [alpha-1,3-]-glycoprotein beta-1,2-N-acetylglucosaminyltransferase I). As indicated in **Figure 6A**, this enzyme is expressed in the mammary tissue and its mRNA level is at its lowest level by the onset of involution. This was further corroborated by western blot analysis of the cytosolic fractions which confirmed the minimal presence of MGAT 1 protein at involution day 1 (**Fig. 6B**).

## Discussion

The dramatic changes in growth, reorganization and function of the mammary gland are prerequisite for milk production and critical for nurturing offspring. These changes are complex and require precise temporal and spatial regulation of many proteins. The significance of proteolytic enzymes at different stages of mammary gland development has been extensively studied; however, CatD's involvement in mammary gland development has remained mostly unexplored.

By employing a mouse model we have established that CatD expression is temporally and spatially regulated during mammary gland development. In the virgin gland CatD expression is mostly intracellular and associated with the lysosomes; however, in the fully differentiated polarized glandular epithelia CatD is mostly associated with the apical surface and is abundantly detected in the milk. This apical presence (and secretion in the milk) is considerably reduced with progression from early to late lactation, and by the onset of involution CatD almost resumes its intracellular location. At involution day 2 CatD immunostaining increases distinctly, and is maintained through days 3 and 4 of involution. By day 4 the glands are clearly regressing with apparent extracellular matrix remodeling, and this continues to day 15, to recapitulate epithelial structure of virgin stage.

The involvement of CatD in mammary gland remodeling was further supported by our in vitro approach (acini formation by MCF-10A in a 3-D organotypic culture). In the early stages of morphogenesis CatD immunoreactivity is detected basolaterally and associated with the matrix juxtaposed to the developing acini. As the acini reaches critical mass and luminal cell death occurs by apoptosis, CatD becomes abundant within the hollowing spheres. Indeed, other matrix-degrading enzymes such as MMP-2,[19] MMP-3[20] and uPA[21] are believed to play a critical role
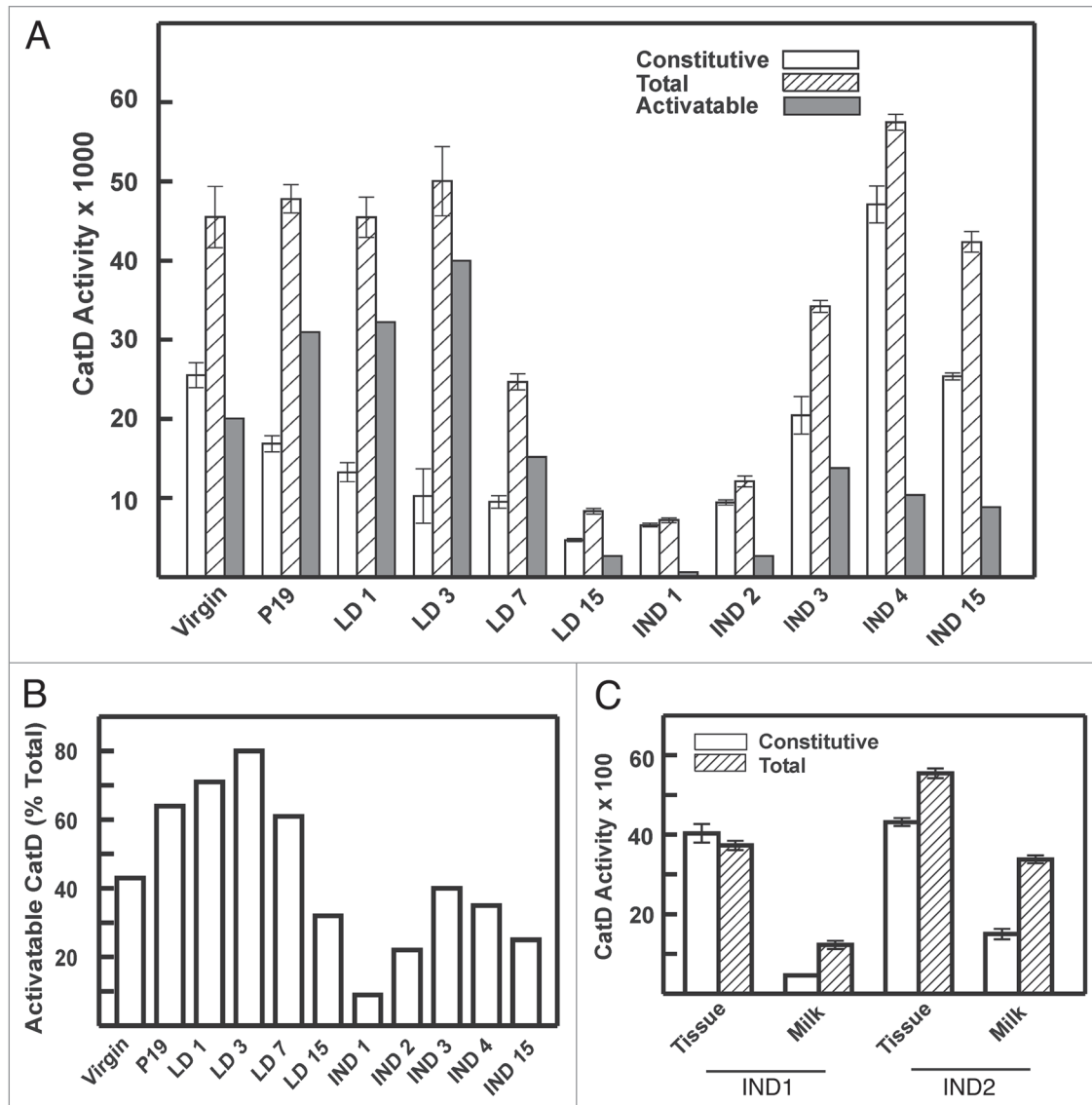
**Figure 4.** CatD enzymatic activity of the post-nuclear cytosolic extracts of the mammary gland is depicted in (A). Protein samples were assayed for either constitutive or total CatD activity as described in the Materials and Methods section. Low pH activatable CatD is constitutive activity subtracted from total activity. Each sample was analyzed in triplicates and the mean values plus standard error of the mean are presented in the graph. (B) Depicts the activatable CatD as % of total. Comparison of total and constitutive CatD activity between tissue and secreted milk at involution days 1 and 2 is presented in (C).

in the remodeling of mouse mammary tissue during involution as well.

Apart from the temporal and spatial expression profile of CatD, our studies also indicate several novel aspects of this endopeptidase at distinct developmental stages. Evidence for differential processing which leads to the preferential presence of specific cleavage products of CatD are observed in lactation and specifically involution stages. Notably, the pro-form (~47 kDa) with slightly higher molecular mass is detected at involution day 1, increases significantly at involution days 2 and 3 but is no longer detectable by day 4, while the active single chain (~41 kDa) CatD is at its highest at involution days 2–4. The involvement of the single chain active CatD in the apoptotic process has been reported previously,[22-25] and it is likely that the abundant

presence of this form in early involution triggers the apoptotic cascade (which is also verified by our immunohistochemical approach) in the gland. In the second stage of involution (days 3 and 4) the mature active forms (32 and 14 kDa CatD) become quite prominent and most likely participate in the degradation of cellular debris and the matrix remodeling process.

Our approach also demonstrates that the distinct changes in protein processing might be critical in customizing CatD enzymatic activity (both constitutive and low pH activatable). Although total CatD activity was comparable in virgin, pregnant and lactating glands, the low pH activatable CatD increased exponentially and was maximal at early lactation. Our finding of the significant response of CatD to low pH at early lactation signifies its important physiological function for an infant's survival during

**Table 1.** Changes in activatable CatD (% total) at different stages of mammary gland development

| Developmental stage | Activatable CatD (% total) |
|---|---|
| Virgin | 43.9 |
| Pregnant | 64.8 |
| Lactation day 1 | 71.0 |
| Lactation day 3 | 80.0 |
| Lactation day 7 | 61.0 |
| Lactation day 15 | 30.0 |
| Involution day 1 | 9.3 |
| Involution day 2 | 22.0 |
| Involution day 3 | 40.0 |
| Involution day 4 | 35.0 |
| Involution day 15 | 23.0 |

early stages of life.[26,27] The low pH of the infant's stomach converts the milk's pro-CatD to the active form to assist in digestion of milk proteins, a premise which is supported by our data that in mid to late lactation the activatable CatD levels drop considerably.

The drop in low pH activatable CatD reaches its maximal level at the onset of involution, and it is important to note that this is not solely due to diminished CatD protein, as both the 47 and 41 kDa CatD components are still detected at considerable levels at involution day 1 and predominantly day 2. Low pH also fails to alter the enzyme activity, which is evident in the corresponding milk samples. A recent study[28] has indicated that involution is associated with nitration of CatD on a tyrosine residue. Although we did not address CatD tyrosine nitration, the slight increase in the apparent molecular mass of the 47 kDa band observed in our model (**Fig. 3**) might reflect nitrated derivatives. In addition, as involution primes the return of the gland to a virgin comparable stage and in anticipation of further pregnancies, delineating the mechanism(s) (i.e., protein nitratase, redox regulation) involved in the de-nitration of tyrosine residues in the mouse mammary gland would be important to pursue.

CatD contains N-linked oligosaccharides (N-glycans) on its asparagin (Asn) residues 70 and 199. In humans these oligosaccharides comprise eight variable high mannose type structures; five are on Asn-70 and the remaining three are on Asn-199.[29,30] The Asn-70 glycans are high mannose structures [3–7 mannose residues attached to the Asn-GlcNAc-GlcNAc core, with one containing a terminal GlcNAc residue (hybrid structure)]. The three oligosaccharides on Asn-199 contain five mannose residues; one has a fucose residue, and the other contains GlcNAc and galactose residues.[9] Our studies also indicate that the 47 and 41 kDa bands exhibit comparable mixed N-glycan profiles at virgin, pregnant and late involution (day 15) stages. However, at involution day 1 the N-glycan structure(s) on the 47 and 41 kDa bands were almost exclusively of the high mannose type; this profile somewhat reverted back to the mixed structures by day 2–3 involution. The change in N-glycan structure results from a significant decline in the mRNA and protein expression of MGAT1, the enzyme which initiates conversion of high-mannose core N-glycans into hybrid and/or complex oligosaccharide

structures.[31] The significance of N-glycan structures in development is just emerging and studies have indicated morphological and developmental abnormalities with defects in N-glycan processing from the high mannose type to hybrid or complex structures.[32,33] In addition, cell type specific function for complex N-glycans has also been documented which signifies their requirement in forming morphologically recognizable bronchia.[34] To our knowledge differential glycosylation of CatD at distinct developmental stages of mammary gland formation has not been reported previously. Whether differential glycosylation of CatD is a determinant of its involvement in apoptosis or is a signal for initiation of involution, remains to be elucidated and is under further investigation in our laboratory.

Collectively, our approach has highlighted a previously unidentified involvement of the multi-faceted endopeptidase CatD in all stages of mammary gland remodeling, and signifies how differential processing of an enzyme (on the protein backbone and oligosaccharide structures) could be the key regulator of its function(s). In addition, secreted CatD in the milk may have a physiological significance for infant survival at early lactation. More importantly, our novel findings indicate for the first time that CatD enzymatic activity is specifically customized for each stage of mammary gland remodeling. It is remarkable that this long discovered lysosomal enzyme continues to proclaim other hidden properties of unique functional relevance. Of significance, deregulated synthesis, secretion and glycosylation of CatD, along with its mitogenic effects are hallmarks of cancer. Thus, the findings reported in this manuscript could potentially assist in deciphering the deregulation of CatD associated with cancer development and metastasis.

## Materials and Methods

**Antibodies.** The following antibodies were utilized for both western blot and immunohistochemical analysis: Goat polyclonal antibody to whey acidic protein (WAP), β-casein and MGAT 1 were from Santa Cruz Biotechnology, Inc.; monoclonal antibodies to Maspin and CatD were from BD Bioscience, and goat polyclonal antibody to mouse CatD and the HRP-labeled secondary antibody to goat were from R&D System. Alexa Fluor labeled secondary antibodies were from Molecular Probe.

**Cell culture.** MCF-10A cells, normal, spontaneously immortalized human mammary epithelial cell line, was maintained in Ham F-12 and DMEM (1:1) growth medium supplemented with 5% horse serum (Invitrogen), epidermal growth factor (20 ng/ml, Peprotech), hydrocortisone (500 ng/ml, Sigma), insulin (10 µg/ml, Sigma) and cholera toxin (100 ng/ml, Sigma).

**3-Dimentional (3-D) basement membrane cultures.** These cultures were established as described by Debnath et al.[16] Briefly, 40 µl of growth factor reduced Matrigel (BD Bioscience) was applied to 8-well glass chamber slides and allowed to solidify at 37°C. MCF-10A cells were harvested, counted and adjusted to 25,000 cells/ml of assay media (same as growth media but with only 2% horse serum). This was further diluted at a 1:1 ratio with a solution of 4% growth factor reduced Matrigel in assay medium to give a final concentration of 12,500 cells/ml in
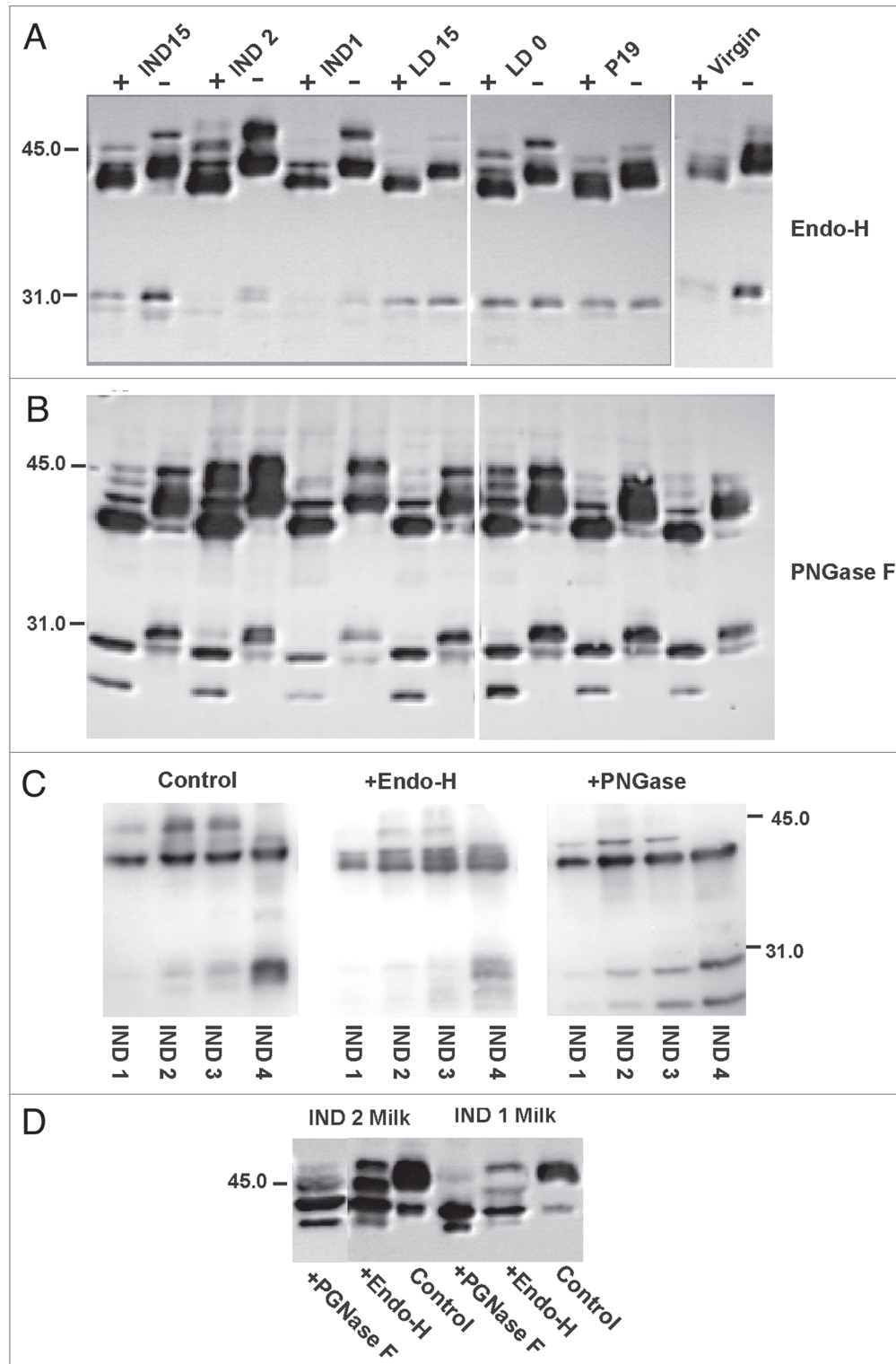
**Figure 5.** N-glycan cleavage profiles resulting from endo-H (A) and PNGase F (B) treatment of the post-nuclear cytosolic extracts of mammary gland from different stages of development. Post-nuclear cytosolic fractions (20 µg for endo-H and 30 µg for PGNase F) were digested with endo-H (0.15 mU) or PNGase F (500 U), as described in the Materials and Methods. The digested material was resolved on a 12.5% SDS-PAGE and subjected to western blot analysis for the detection of CatD reactive fragments. For comparison purposes cytosolic extracts of different involution days (1–4) are depicted separately (C). Milk protein samples from involution days 1 and 2 (50 and 12 µg total protein, respectively) were similarly treated and analyzed (D). Variable total protein in the milk samples was to compensate for the low abundance of CatD in involution day 1 compared to day 2. Molecular weight markers are indicated for each blot.
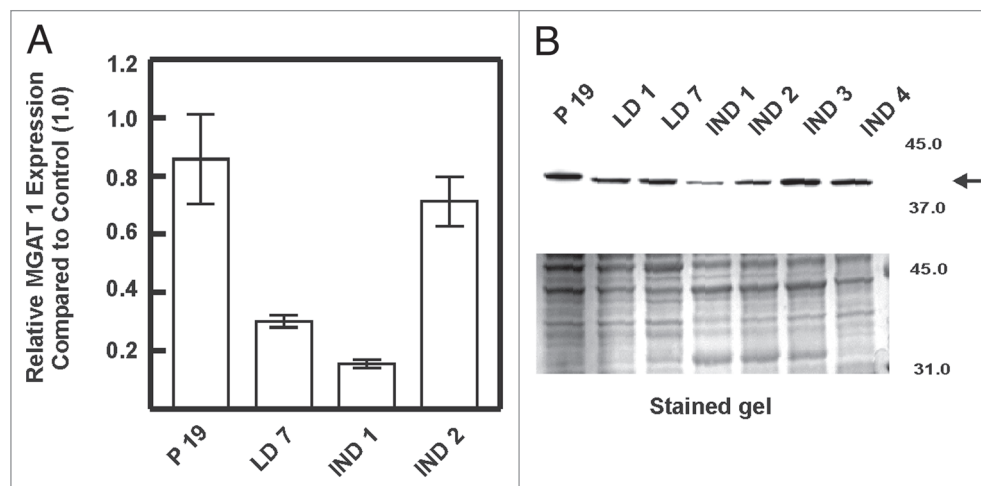
**Figure 6.** Expression profile of MGAT 1 gene (A) and protein (B) at specific remodeling stages of mammary gland development. Gene expression was analyzed by real-time PCR using primer probes for mouse MGAT 1, and the protein profile was examined using SDS-PAGE on a 4–20% acrylamide gel. For the loading control, a picture of the stained gel following the transfer is included. The molecular weight markers are indicated for the blot and the stained gel. Arrow indicates the position of MGAT 1.

2% Matrigel in assay media. 400 µl (equal to 5,000 cells) was overlaid on the Matrigel blocks and cultures were maintained at 37°C, 5% $CO_2$, and were fed every 4 days. Cultures were fixed in 2% formaldehyde (pH 7.4) and permeabilized, blocked and treated with antibodies to CatD and Maspin at 1:250 and 1:200 dilution in blocking buffer. After several washes the antibody-antigen complex was detected using Alexa Fluor labeled secondary antibodies at 1:200 (Molecular Probe). Nuclei were counterstained with 4'-6'-diamidino-2-phenylindole dihydrochloride (DAPI). Slides were mounted using Gelvatol anti-fade and viewed by confocal microscopy using the Zeiss LSM-510 META confocal laser scanning microscope.

**Animals.** Female C57BL mice (Harlan, Indianapolis, IN) were used at the following stages of development: Virgin (6–8 weeks old, V), pregnant (19 days of pregnancy, P19), lactating (1, 3, 7 and 15 days of lactation, LD), post-lactation/involution (1–4, 7 and 15 days after the removal of pups on day 15th of lactation, IND). The animals were euthanized with ketamine and xylazine (80 mg/kg + 10 mg/kg, ip) and sacrificed by cervical dislocation under deep anesthesia. Pectoral and inguinal groups of mammary glands were removed, and immediately frozen in liquid nitrogen for later use or were fixed in 10% neutral buffered formalin, processed in a tissue processor and embedded in paraffin for immunohistochemical analysis. Six sets of mice at each stage of development were employed in these studies.

All the animal protocols were reviewed and approved by Institutional Animal Care and Use Committee of Children's Memorial Research Center and Northwestern University Feinberg School of Medicine, which is AALAC accredited.

**Milk collection.** Collection of milk samples was achievable only from involution days 1 and 2; they were centrifuged, the lipid layer was removed, and the remaining supernatant was used for western blot and enzyme activity assays.

**Tissue preparation and western blot analysis.** The mammary tissues (inguinal glands 5–6) were removed, chilled in liquid nitrogen and were either used immediately or kept frozen at -80 degrees for later use. The frozen tissue was pulverized in pre-chilled mortar and pestle and homogenized in buffer A (10 mM HEPES buffer pH 7.9 containing 10 mM NaCl, 1 mM DTT, 10% glycerol, 15 mM $MgCl_2$, 0.2 mM EDTA, 0.1% NP40, protease inhibitor cocktail). The homogenate was subjected to 3 freeze-thaw cycles, passed several times through a 28-gauge needle and centrifuged (4,500x g, 10 min) to yield a post-nuclear cytosolic fraction which was used for general screening. The protein content of the fraction was determined using BCA reagent, and 20 µg total protein was subjected to SDS-PAGE analysis under reduced conditions. The proteins were then transblotted to PDF membrane, blocked with 5% dried milk in 0.1 M Tris, 0.2 M NaCl buffer (pH 7.4) containing 0.1% Tween 20 (TSBT) and probed with respective antibodies. Antigen-antibody complexes were visualized by employing peroxidase labeled secondary antibodies and ECL detection system (GE Health Care).

**CatD activity assay.** The assay was performed in 96-well black ELISA plates as described previously.[17] Briefly, the post-nuclear cytosolic fraction (20 µg total protein) was utilized to assess the level of constitutively active (measured without activation at low pH) and activatable (after activation at pH 3.5, 30 min, 37°C) CatD at different stages of development. Activated and non-activated protein samples were taken in reaction buffer (0.1 M sodium acetate, 5 mM DDT, 1 mM EDTA, pH 5.5, final volume of 100 µl) at room temperature and in the presence or absence of pepstatin (specific aspartyl protease inhibitor). Each sample was assayed in triplicate and the protease activity of CatD was measured by the addition (10 µM) of the fluorogenic peptide substrate Mca-P-L-G-L-Dpa-A-R-$NH_2$ (R&D Systems, Inc.,) using the fluorescence plate reader FluoStar Optima (BMG Labteck GmbH, Durham, NC) with excitation and emission of 320 nm and 405 nm, respectively. Error bars indicate standard deviation of the mean.

**Analysis of CatD oligosaccharides.** To examine the possible alteration(s) in the N-glycan profile of CatD at different stages of remodeling we employed two enzymes endo-β-N-actelyglucosaminidase H (endo-H, recombinant protein from *Streptomyces Plicatus,* expressed in *E. Coli)* from Prozyme® and N-glycanase (PNGase F, purified from *Flavobacterium meningosepticum)* from New England, Biolabs Inc. Post-nuclear cytosolic fractions and milk samples from days 1 and 2 involution were digested with endo-H (0.15 mU) or PNGase F (500 U) according to established protocols. The digested material was subjected to SDS-PAGE and western blot analysis and probed with anti-mouse CatD.

**Real-time PCR.** Total RNA was isolated from frozen mammary tissue using Trizol RNA isolation reagent (Life Technologies, Inc.,) according to manufacturer's specifications. Reverse transcription of the total RNA was performed in a Robocycler gradient 96 thermocycler (Stratagene, La Jolla, CA) using the Advantage PCR kit according to the manufacturer's instructions (Clontech, Palo Alto, CA). PCR was performed on a 7500 Real Time PCR System (Applied Biosystems, Foster City, CA) using TaqMan® gene expression primer/probe sets (Mouse MGAT1: Mm00487690_m1, Applied Biosystems). Briefly, 5 μl cDNA, 1.25 μl 20X Assays-on-Demand Gene Expression Assay Mix and 12.5 μl 2X TaqMan® Universal PCR Master Mix in a total of 25 μl were amplified with the following thermocycler protocol: 1 cycle at 50°C for 2 min; 1 cycle at 95°C for 10 min; and 33 cycles at 95°C for 15 seconds/60°C for 1 min. All data were analyzed with the Sequence Detection Software (version 1.2.3, Applied Biosystems). The expression of target gene was normalized to an endogenous control gene (18S rRNA:Hs99999901_s1 large ribosomal protein primer/probe set, Applied Biosystems).

Each sample was performed in triplicate and each experiment was repeated three times.

**Immunohistochemistry.** Expression of proteins of interest was examined by immunohistochemical analyses of the formalin fixed, paraffin embedded mammary tissue. Sections (4 μm) were deparaffinized, subjected to citrate buffer (pH 6.0) water bath antigen retrieval and blocked (endogenous peroxidase, protein, Avidin and Biotin [Avidin/Biotin blocking kit, Vector Laboratories, Inc., Burlingame, CA]) prior to primary antibody treatment as described previously.[18] The staining was performed on a Microm HMS 710i Automated Immunostainer (ThermoFisher Scientific/Richard-Allan Scientific) with antibodies against CatD and WAP at concentrations depicted in the figure legends. The secondary biotinylated anti-goat was from Biocare Medical and used according to the manufacture's instruction, followed by treatment with streptavidin peroxidase reagent (ThermoFisher Scientific/Lab Vision). The color was developed using DAB⁺ substrate (ThermoFisher Scientific/Lab Vision); the slides were counterstained with Mayer's Hematoxylin (Dako), dehydrated in ethanol and xylene and coverslipped with permanent mounting medium.

Normal goat IgG (at similar concentrations to primary antibody) served as a negative control. Slides were viewed and the area of interest recorded using a Leica DM 4000B microscope attached to a Leica DFC 480 5.0 Mega pixel CCD camera.

### Note

Supplementry materials can be found at:
www.landesbioscience.com/supplement/MargaryanCBT10-5-sup.pdf

### References

1. Humphreys RC, Krajewska M, Krnacik S, Jaeger R, Weiher H, Krajewski S, et al. Apoptosis in the terminal endbud of the murine mammary gland: a mechanism of ductal morphogenesis. Development 1996; 122:4013-22.

2. Li B, Kittrell FS, Medina D, Rosen JM. Delay of dimethylbenz[a]anthracene-induced mammary tumorigenesis in transgenic mice by apoptosis induced by an unusual mutant p53 protein. Mol Carcinog 1995; 14:75-83.

3. Rosen JM, O'Neal DL, McHugh JE, Comstock JP. Progesterone-mediated inhibition of casein mRNA and polysomal casein synthesis in the rat mammary gland during pregnancy. Biochemistry 1978; 17:290-7.

4. Deiss LP, Galinka H, Berissi H, Cohen O, Kimchi A. Cathepsin D protease mediates programmed cell death induced by interferon-gamma, Fas/APO-1 and TNF-alpha. EMBO J 1996*;* 15*:*3861-70.

5. Feng Z, Marti A, Jehn B, Altermatt HJ, Chicaiza G, Jaggi R. Glucocorticoid and progesterone inhibit involution and programmed cell death in the mouse mammary gland. J Cell Biol 1995; 131:1095-103.

6. Lund LR, Rømer J, Thomasset N, Solberg H, Pyke C, Bissell MJ, et al. Two distinct phases of apoptosis in mammary gland involution: proteinase-independent and-dependent pathways. Development 1996; 122:181-93.

7. Stein T, Salomonis N, Gusterson BA. Mammary gland involution as a multi-step process. J Mammary Gland Biol Neoplasia 2007; 12:25-35.

8. Von Figura MC, Hasilik A. Lysosomal enzymes and their receptors. Annual Rev Biochem 1986; 55:167-93.

9. Gieselmann V, Pohlmann R, Hasilik A, von Figura K. Biosynthesis and transport of cathepsin D in cultured human fibroblasts. J Cell Biol 1983; 97:1-5.

10. Cantor AB, Baransk TJ, Kornfeld S. Lysosomal enzyme phosphorylation II. Protein recognition determinants in either lobe of procathepsin D are sufficient for phosphorylation of both the amino and carboxyl lobe oligosaccharides. J Biol Chem 1992; 267:23349-56.

11. Biddere N, Lorenzo HK, Carmona S, Laforge M, Harper F, Dumont C, et al. Cathepsin D triggers Bax activation, resulting in selective apoptosis-inducing factor relocation in T lymphocytes entering the early commitment phase to apoptosis. J Biol Chem 2003; 278:31401-11.

12. Miller DK, Griffiths E, Lenard J, Firestone RA. Cell killing by lysosomotrophic agents. J Cell Biol 1983; 97:1841-51.

13. Saftig P, Hetman M, Schmahl W, Weber K, Heine L, Mossmann H. Mice deficient for the lysosomal proteinase cathepsin D exhibit progressive atrophy of the intestinal mucosa and profound destruction of lymphoid cells. EMBO J 1995; 14:3599-608.

14. Koike M, Shibata M, Waguri S, Yoshimura K, Tanida I, Kominami E, et al. Participation of autophagy in storage of lysosomes in neurons from mouse models of neuronal ceroid-lipofuscinoses (Batten disease). Am J Pathol 2005; 167:1713-28.

15. Kroemer G, Jaattela M. Lysosomes and autophagy in cell death control. Nat Rev Cancer 2005; 5:886-97.

16. Debnath J, Muthuswamy SK, Brugge JS. Morphogenesis and oncogenesis of MCF-10A mammary acini grown in three-dimentional basement membrane cultures. Methods 2003; 30:256-68.

17. Khalkhali-Ellis Z, Abbott DE, Bailey CM, Goossens W, Margaryan NV, Gluck SL, et al. IFNgamma regulation of vacuolar pH, cathepsin D processing and autophagy in mammary epithelial cells. J Cell Biochem 2008*;* 105:208-18.

18. Khalkhali-Ellis Z, Christian AL, Kirschmann DA, Edwards EM, Rezaie-Thompson M, Vasef MA, et al. Regulating the tumor suppressor gene maspin in breast cancer cells: a potential mechanism for the anticancer properties of tamoxifen. Clin Cancer Res 2004; 10:449-54.

19. Dickson SR, Warburton MJ. Enhanced synthesis of gelatinase and stromelysin by myoepithelial cells during involution of the rat mammary gland. J Histochem Cytochem 1992; 40:697-703.

20. de la Cruz L, Steffgen K, Martin A, McGee C, Hathaway H. Apoptosis and involution in the mammary gland are altered in mice lacking a novel receptor, β1,4-galactosyltransferase I. Dev Biol 2004; 272:286-309.

21. Busso N, Huarte J, Vassalli JD, Sappino AP, Belin D. Plasminogen activators in the mouse mammary gland. Decreased expression during lactation. J Biol Chem 1989*;* 264:7455-7.

22. Deis RP, Delouis C. Lactogenesis is induced by ovariectomy in pregnant rats and its regulation by oesterogen and progesterone. J Steroid Biochem 1983; 18:687-90.

23. Wille A, Gerber A, Heimburg A, Reisenauer A, Peters C, Saftig P. Cathepsin L is involved in cathepsin D processing and regulation of apoptosis in A549 human lung epithelial cells. Biol Chem 2004; 385:665-70.

24. Quarrie LH, Addey CV, Wilde CJ. Apoptosis in lactating and involuting mouse mammary tissue demonstrated by nick-end DNA labeling. Cell Tissue Res 1995; 281:413-9.

25. Monks J, Rosner D, Geske FJ, Lehman L, Hanson L, Neville MC, et al. Epithelial cells are phagocytes: apoptotic epithelial cells are engulfed by mammary alveolar epithelial cells and repress inflammatory mediator release. Cell Death and Dif 2005; 12:107-14.

26. Davies PH, Messer M. Intestinal cathepsin B and D activities of suckling rats. Biol Neonate 1984; 45:197-202.

27. Britton JR, Koldovský O. Development of luminal protein digestion in suckling and weanling rats. Biol Neonate 1988; 53:39-46.

28. Zaragoza R, Torres L, Garcia C, Eroles P, Corrales F, Bosch A, et al. Nitration of cathepsin D enhances its proteolytic activity during mammary gland remodeling after lactation. Biochem J 2009; 419:279-88.

29. Hasilik A, Neufeld E. Biosynthesis of lysosomal enzymes in fibroblasts. Phosphorylation of mannose residues. J Biol Chem 1980; 255:4946-50.

30. Minarowska A, Gacko M, Karwowska A, Minarowski L. Human cathepsin D. Folia Histochem Cytobiol 2008; 46:23-38.

31. Kumar R, Yang J, Larsen RD, Stanley P. Cloning and expression of N-acetylglucosaminyltransferase I, the medial Golgi transferase that initiates complex N-linked carbohydrate formation. Proc Nat Acad Sci USA 1990; 87:9948-52.

32. Ioffe E, Stanley P. Mice lacking N-acetylglucosaminyltransferase activity died at midgestation, revealing an essential role for complex or hybrid N-linked carbohydrate. Proc Nat Acad Sci USA 1994; 91:728-32.

33. Metzler M, Gertz A, Sarkar M, Schachter H, Schrader JW, Marth JD. Complex asparagine-linked oligosaccharides are required for morphogenic events during post-implantation development. EMBO J 1994; 13:2056-65.

34. Ioffe E, Yun L, Stanley P. Essential role for complex N-glycans in forming organized layer of bronchial epithelium. Proc Nat Acad Sci USA 1996; 93:11041-46.